EXAFS study of Sr doped $Y_{0.4}Pr_{0.6}Ba_2Cu_3O_{7-\delta}$*

T S Anvekar, K R Priolkar, V G Sathe[1], A V Pimpale[1], P R Sarode & V N Kamat Dalal[2]

Department of Physics, Goa University, Taleigao Plateau, Goa 403 206

[1]Inter University Consortium for DAE Facilities, University Campus, Khandwa Road, Indore 452 001

[2]Department of Chemistry, Goa University, Taleigao Plateau, Goa 403 206

The Cu K-edge extended X-ray absorption fine structure (EXAFS) studies in $YBa_2Cu_3O_{7-\delta}$ and $Y_{0.4}Pr_{0.6}Ba_{2-x}Sr_xCu_3O_{7-\delta}$ with $0 \le x \le 1.25$ have been carried out to examine the changes in near neighbour environment of Cu as a function of Sr doping. There is a sudden shift of apical oxygen O(4) towards the CuO planes in compounds wherein superconductivity is restored. This contraction in the Cu(2)-O(4) bond length seems to weaken the Pr-O hybridization and thereby restoring superconductivity. Infrared absorption studies on these compounds also support this picture.

1 Introduction

Suppression of superconductivity in Pr doped $RBa_2Cu_3O_7$ (123) system, (R is a rare earth except Ce) and its subsequent revival by Sr doping at Ba site has attracted a lot of attention in recent past[1-4]. Revival of superconductivity was first reported by Cao et al.[2] in $Y_{0.4}Pr_{0.6}Ba_2Cu_3O_{7-\delta}$ and was attributed to ion size effect at Ba site. Sr, being a smaller ion than Ba, at larger doping concentrations decreases the Cu-O (2,3) (planar oxygen) distance and increases the Pr-O (2,3) distance. This reduces the Pr-O covalency thereby releasing the localized holes and reviving the superconductivity. The photo-emission and Raman studies on the same series[5] showed that Sr substitution for Ba leads to an enhanced Ba/Sr-O interaction coupled with weakening of Pr-O covalency. Zelenay et al.[3] also hinted at weakening of hybridization between Pr(4f) -O(2$p\pi$) orbitals along with reduction of disorder in the chains as the cause of revival of superconductivity in $Nd_{0.7}Pr_{0.3}Ba_{2-x}Sr_xCu_3O_{7-\delta}$. The weakening of hybridization was brought about by Sr probably by weakening the anti-ferromagnetic interactions of Pr in the 123 lattice.

In order to study the local environment of copper ions in Sr doped samples, extended X-ray absorption fine structure (EXAFS) spectra at the Cu K-edge were recorded in these materials. The Cu-O bond lengths were obtained from the analysis of the EXAFS data. The changes in the local structure around copper ions were determined as a function of dopant concentrations.

2 Experimental Details

The compounds with nominal composition, $Y_{0.4}Pr_{0.6}Ba_{2-x}Sr_xCu_3O_{7-\delta}$ with $0 \le x \le 1.25$ were prepared by the standard ceramic procedure. Highly pure ingredients, in appropriate stoichiometric ratios were thoroughly mixed in agate mortar and pestle. The mixtures were calcined in air several times with intermittent grindings. The calcined samples were cold pressed and annealed in oxygen for 24 hr at 935 °C and for another 24 hr at 600 °C. The samples were then characterized by X-ray diffraction using Rigaku X-ray diffractometer (D Max II-C) and four probe resistivity measurements. The diffraction patterns indicated that samples were essentially single phase with traces of impurity phases at higher values of x ($\ge$ 0.75). Resistivity measurements showed restoration of superconductivity with increasing Sr concentration. Oxygen content was determined by iodometric titration. The X-ray diffraction, resistivity and iodometry results are presented in Table 1.

Extended X-ray absorption fine structure (EXAFS) at the Cu K-edge of $Y_{0.4}Pr_{0.6}Ba_{2-x}Sr_xCu_3O_{7-\delta}$ (YPBS123) system was recorded at room temperature using Johansson type bent crystal X-ray

spectrometer with a Si(311) crystal plane as monochromator and white radiation from rotating anode X-ray generator. The total number of incident photons recorded was $\cong 3 \times 10^5$ at each data point. The energy was referenced to the Cu $K_{\beta 1}$ emission line, which was assigned the tabulated energy of 8905.14 eV(Ref. 6). The cubic spline interpolation for generating equidistant points in k-space along with adequate smoothing to remove the noise from the raw data was employed. The data analysis was done using UWXAFS 3.0 (Refs. 7-10).

Table 1 — Lattice parameters (a, b, c), unit cell volume (V), critical temperature (T_c) and oxygen content $(7-\delta)$ for $YBa_2Cu_3O_{7-\delta}$ and $Y_{0.4}Pr_{0.6}Ba_{2-x}Sr_xCu_3O_{7-\delta}$

X	$a(\text{Å})$	$b(\text{Å})$	$c(\text{Å})$	$V(\text{Å}^3)$	(K)	$7-\delta$
Y-123	3.826	3.898	11.694	174.40	89	6.89
0.00	3.856	3.902	11.706	176.12	NSC	6.80
0.50	3.852	3.880	11.640	173.96	NSC	6.67
0.75	3.872	3.872	11.616	174.15	NSC	6.90
1.00	3.864	3.864	11.592	173.07	NSC	6.85
1.25	3.852	3.862	11.556	171.46	19	6.92

NSC – Non-superconducting

The IR spectra of the series have been studied at room temperature in the range of 400 to 800 cm⁻¹ using a Shimadzu FTIR spectrophotometer.

3 Results and Discussion

Fig. 1 shows Cu K-edge spectra of YPBS123 ($x = 0$ and 1.25) and $YBa_2Cu_3O_{7-\delta}$ (Y123) along with the model compounds, Cu metal and CuO. The Y123 spectrum is similar to that reported in literature[11]. The spectra of Sr doped compounds are quite similar to that of Y123 indicating thereby a similar environment for Cu ions in all the 123 compounds. The EXAFS of CuO, Y123 and YPBS123 ($x = 0$ and 1.25) is shown in Fig. 2. The spectra are expectedly similar in nature as in all the 123 compounds Cu is surrounded by oxygen atoms in the first coordination shell. The magnitudes of Fourier transforms (FT) of $\chi(k)$ along with fitted curves are shown in Fig. 3. The fitting was done in the region R = 1–2 Å. The FT of CuO exhibits a peak corresponding to 4 oxygen atoms at an average distance of 1.9 Å. It may be noted here that the distances mentioned in the text and tables are corrected for phase shift and it is because of this phase shift the peaks in Fig. 3 appear at lower distances as at about 1.6 Å in the present case. A peak at about the same distance is also seen in the

Y123 FT spectrum. Y123 has an orthorhombic structure with a single formula unit-per-unit cell.
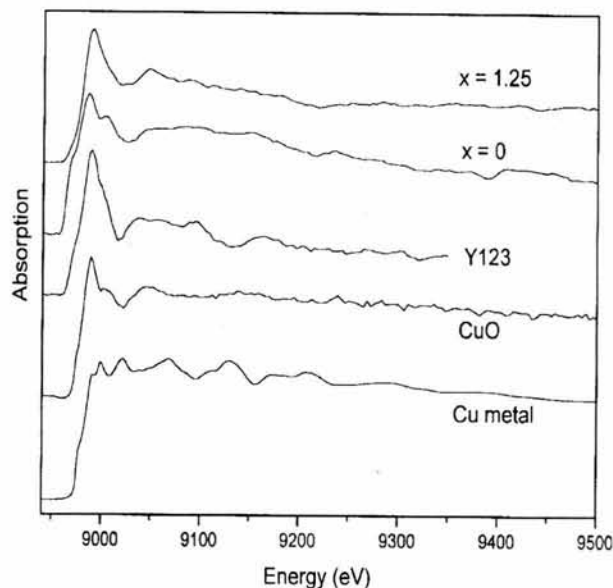

Fig. 1 — Cu K-edge EXAFS in Cu metal, CuO, Y123 and $Y_{0.4}Pr_{0.6}Ba_{2-x}Sr_xCu_3O_{7-\delta}$
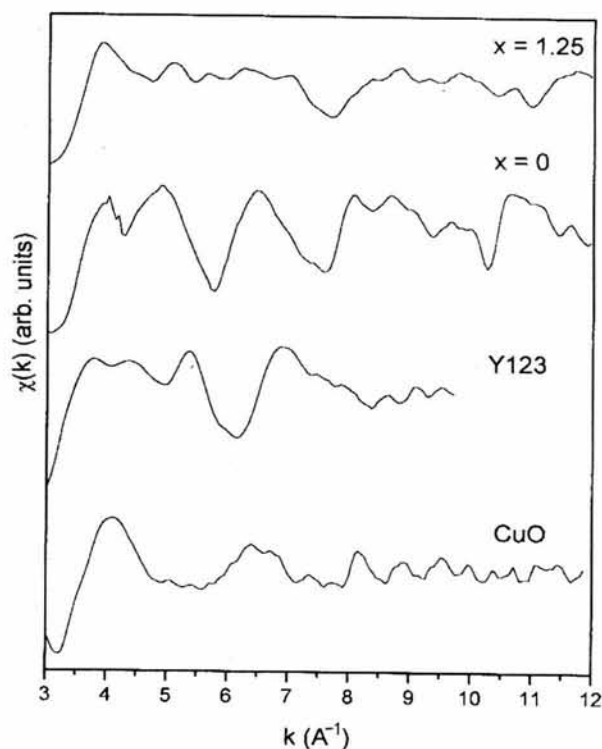
$(x = 0$ and 1.25)

Fig. 2 — EXAFS function $\chi(k)$ versus k in CuO, Y123 and $Y_{0.4}Pr_{0.6}Ba_{2-x}Sr_xCu_3O_{7-\delta}$

$(x = 0$ and 1.25)

There are two distinct copper sites in this material: the $Cu(1)$ sites are 4-fold coordinated by O atoms, also known as the chain sites because of the $Cu(1)$-$O(1)$ chains that they form with each other, and the square pyramidal $Cu(2)$ sites are 5-fold coordinated by O atoms also called the planar sites due to Cu-O planes formed with the $O(2)$ and $O(3)$ atoms. The fifth oxygen, $O(4)$, coordinated to $Cu(2)$ is called as apical oxygen or bridging oxygen as it forms a bridge between $Cu(1)$ and $Cu(2)$ atoms. The planes are slightly dimpled with the O atoms displaced from the central plane by about 0.266 Å. This gives five different Cu-O distances as discerned by neutron diffraction[12]. The broad peak at 1.9 Å (1.6 Å in Fig. 3 due to effect of phase shift) is a sum of all the five Cu-O correlations. The authors have done three-distance fit with some reasonable constraint to reduce parameter correlation instabilities. The three-distance fit consists of the following correlations $Cu(1)$-$O(4)$, weighted average of $Cu(1)$-$O(1)$, $Cu(2)$-$O(2)$ and $Cu(2)$-$O(3)$ and $Cu(2)$-$O(4)$. Since there are two five-fold coordinated Cu sites and one four-fold coordinated Cu site in the Y-123 unit cell the weighted average of the number of nearest neighbour oxygen atoms is 4.67. The fitting parameters obtained for Y123 were used as input parameters for the Sr doped compounds. The results obtained are presented in Table 2.

Table 2 — Cu-O bond distances in Å of $YBa_2Cu_3O_{7-\delta}$ and $Y_{0.4}Pr_{0.6}Ba_{2-x}Sr_xCu_3O_{7-\delta}$ system

X	$Cu(1)$-$O(4)$	Average of $Cu(1)$-$O(1)$, $Cu(2)$-$O(2)$, $Cu(2)$-$O(3)$	$Cu(2)$-$O(4)$
Y-123	1.85(2)	1.91(1)	2.30(1)
0.00	1.90(1)	1.94(2)	2.32(2)
0.50	1.82(2)	1.94(2)	2.31(2)
0.75	1.81(3)	1.91(2)	2.30(1)
1.00	1.82(1)	1.90(1)	2.25(1)
1.25	1.83(2)	1.90(2)	2.24(1)

(Values in bracket indicate uncertainties in the last digit)

It can be seen from the Table 2 that, though there is an extremely small variation in bond length there is a general contraction of all the Cu-O bonds on Sr doping which is as expected. It is believed that in the Pr doped samples, the suppression of superconductivity takes place due to decrease in Cu-O hybridization brought about by the localization of holes by Pr. Cao et al.[13] in their paper on the same

compounds have suggested that Sr substitution for Ba in the Pr doped non-superconducting system leads to an enhanced Ba/Sr-O interaction coupled with weakening of Pr-O covalency. This reduces the Cu-$O(2,3)$ bond lengths which result in increased Cu-O hybridization and hence appearance of superconductivity in these compounds. Our results also show that the average bond length of $Cu(1)$-$O(1)$, $Cu(2)$-$O(2)$ and $Cu(2)$-$O(3)$ decreases with increasing Sr concentration but just within the error limit. Another interesting result observed is, the decrease in $Cu(2)$-$O(4)$ bond length. This implies that, the contraction of c-axis results in shift of the apical oxygen and of the Ba(Sr) ions towards the CuO_2 planes. The decrease in bond length however is not monotonic, there is sudden jump from 2.30 ± 0.01 to 2.25 ± 0.01 Å as the Sr content is increased from 0.75 to 1.0 (the Sr concentration at which the sample becomes superconducting).
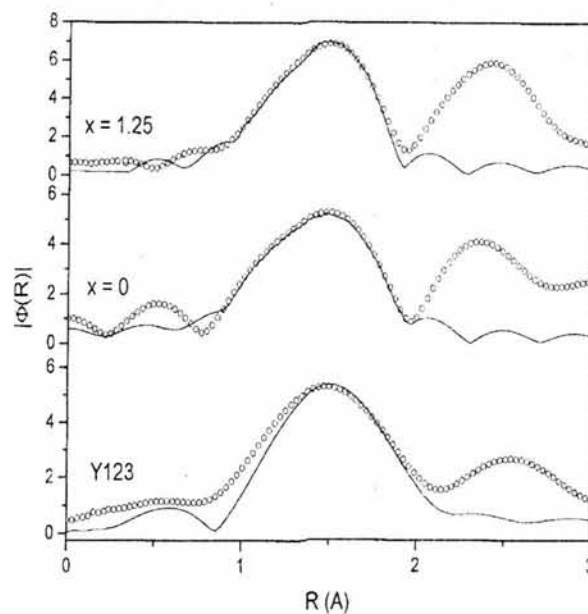

Fig. 3 — Magnitude of Fourier Transform $\phi(R)$ versus R in Y123 and $Y_{0.4}Pr_{0.6}Ba_{2-x}Sr_xCu_3O_{7-\delta}$

($x = 0$ and 1.25). Experimental data is shown as circles while solid line indicates fitted curve

Infrared absorption spectra of these compounds are shown in Fig. 4. The Y123 spectra in the region from 400 to 800 cm^{-1} show three IR active modes: the peak in the vicinity of 617 cm^{-1} can be assigned to $Cu(1)$-$O(4)$ vibrations, the peak around 590 cm^{-1} due to $Cu(2)$-$O(2)$ vibrations[14] and the peak around 470 cm^{-1} because of $Cu(2)$-$O(3)$ vibrations[15]. When

Pr is introduced up to 60% in place of Y, the sample shows semiconducting character that is reflected by the IR spectrum of this sample. The first two of the three aforementioned bands show very little change in their positions. However, it may be noted that the band at 617 cm^{-1} considerably weakens in intensity.
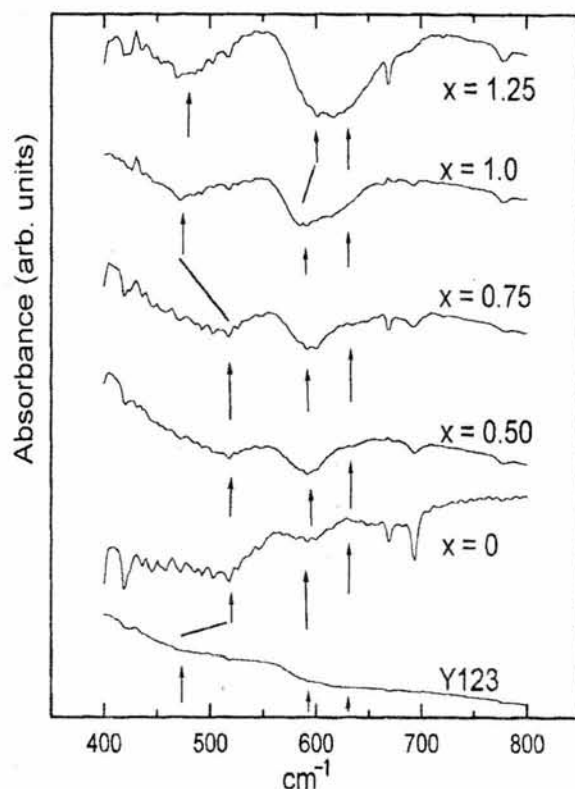

Fig. 4 — Infrared absorption spectra of Y123 and $Y_{0.4}Pr_{0.6}Ba_{2-x}Sr_xCu_3O_{7-\delta}$ ($0 \leq x \leq 1.25$)

But the third band i.e. 470 cm^{-1} band, shows drastic shift in its position in the spectrum. This band moves towards higher energy side at about 510 cm^{-1}. This could be possible because there is a change in ionic size of (R) and hence change in lattice constants, which influence the lattice vibrational modes. Further with Sr substitution at the Ba site the intensity of 617 cm^{-1} band decreases appreciably with a disappearance at $x = 0.5$ and 0.75 samples. However, no change in its position of the 510 cm^{-1} band is observed. The apical oxygen O(4) is the nearest neighbour of Ba. Any site disorder would strongly affect the O(4) atoms. Substitution of Sr in place of Ba perhaps introduces a site disorder also believed to be one of the likely causes of suppression of T_c in the $YBa_{2-x}Sr_xCu_3O_{7-\delta}$ sample[16]. This site disorder may be the reason for

considerable weakening of the Cu(1)-O(4) stretch which points to disappearance of 617 cm^{-1} band. When the Sr content increases to more than 50 at % superconductivity reappears and with it two interesting changes occur in the IR spectra. The 470 cm^{-1} band in the Y-123 sample which had moved to 510 cm^{-1} in the non-superconducting samples, moves back to its original position of 470 cm^{-1}. Also the Cu(1)-O(4) stretch reappears at a slightly lower frequency (614 cm^{-1}) in $x = 1.0$ sample but moves up to 617 cm^{-1} in the $x = 1.25$ sample. This agrees well with the changes in the Cu-O bond lengths, especially the Cu(2)-O(4) bond length. The shift of apical oxygen towards the Cu-O planes at higher Sr concentrations probably leads to the increase of Cu-O hybridization thereby resulting in restoration of superconductivity.

4 Conclusion

The results of the present study imply that the contraction of c-axis in Sr doped $Y_{0.4}Pr_{0.6}Ba_2Cu_3O_{7-\delta}$ is due to the shift of the apical oxygen O(4) towards the CuO$_2$ planes which decreases the Cu(2)-O(4) bond length. This shift seems to weaken the Pr-O(2,3) hybridization thereby restoring the T_c. This is also well correlated by reappearance of 470 and 614 cm^{-1} stretching modes in the superconducting Sr doped samples.

Acknowledgements

References

1   Chen J M, Liu R S, Lin J G et al., *Phys Rev B*, 55 (1997) 14586.

2   Cao G H, Qian Y T, Li X J et al., *J Phys Condens Matter*, 7 (1995) L287.

3   Zelenay I, Das A & Suryanarayanan R, *Phys Lett A*, 222 (1996) 451.

4   Das A & Suryanarayanan R, *Phys Status Solidi (b)*, 191 (1995) K5.

5   Cao G, Qian Y, Zhu J et al., *J Phys Chem Solids*, 58 (1997) 769.

6   Beerden J A, *X-ray wavelengths and X-ray atomic energy levels*, NSRDS-NBS, 14, 1967.

7   Mustre de Leon J, Rehr J J, Zabinsky S I & Albers R C, *Phys Rev B*, 44 (1991) 4146.

8   Rehr J J, Albers R C & Zabinsky S I, *Phys Rev Lett*, 69 (1992) 3397.

9   Rehr J J, Mustre de Leon J, Zabinsky S I & Albers R C, *J Am Chem Soc*, 113 (1991) 5135.

10 Zabinsky S I, Rehr J J, Ankudinov A *et al.*, *Phys Rev B*, (1995) 2995.

11 Sacchi M, Corni F, Antonini G M *et al.*, *Z Phys B, Condens Matter*, 72 (1988) 335.

12 Beno M A, Soderholm L, Capone D W *et al.*, *Appl Phys Lett*, 51 (1987) 57.

13 Cao G H, Qian Y T, Li X J *et al.*, *Phys Lett A*, 196 (1994) 263.

14 Crawford M K, Farneth W E, McCarron III E M & Bordia R K, *Phys Rev B*, 38 (1988) 11382.

15 Feile Rudolf, *Physica C*, 159 (1989) 1.

16 Veal B W, Kwok W K, Umezava A *et al.*, *Appl Phys Lett*, 51 (1987) 279.